SURFACE AND INTERFACE ANALYSIS
Surf. Interface Anal. 2003; **35**: 998–1003
Published online in Wiley InterScience (www.interscience.wiley.com). DOI: 10.1002/sia.1638

SIA

Study of the electronic and atomic structure of thermally treated $SrTiO_3$(110) surfaces

A. Gunhold,[1] L. Beuermann,[1] K. Gömann,[2] G. Borchardt,[2] V. Kempter,[1] W. Maus-Friedrichs,[1]* S. Piskunov,[3] E. A. Kotomin[4] and S. Dorfman[5]

[1] Institut für Physik und Physikalische Technologien, Technische Universität Clausthal, Leibnizstr. 4, D-38678 Clausthal-Zellerfeld, Germany
[2] Institut für Metallurgie, Technische Universität Clausthal, Robert-Koch-Str. 42, D-38678 Clausthal-Zellerfeld, Germany
[3] Fachbereich Physik, Universität Osnabrück, Barbarastr. 7, D-49069 Osnabrück, Germany
[4] Institute of Solid State Physics, University of Latvia, Kengaraga 8, LV-1063 Riga, Latvia, and Max Planck Institut für Festkörperforschung, Heisenbergstr. 1, D-70569 Stuttgart, Germany
[5] Department of Physics, Israel Institute of Technology — Technion, 32000 Haifa, Israel

Received 26 June 2003; Revised 19 September 2003; Accepted 20 September 2003

The electronic structure of heated $SrTiO_3$(110) surfaces was investigated with metastable impact electron spectroscopy and ultraviolet photoelectron spectroscopy (He(I)). Scanning tunnelling microscopy and atomic force microscopy (AFM) were used to study the topology of the surface. The crystals were heated up to 1000 °C under reducing conditions in ultrahigh vacuum or under oxidizing conditions in synthetic air for 1 h, respectively. Under both conditions microfacetting of the surface is observed. The experimental results are compared with *ab initio* Hartree–Fock calculations, also presented here, carried out for both ideal and reconstructed $SrTiO_3$(110) surfaces. The results give direct evidence for Ti termination of the faceted TiO_2 rows. Copyright © 2003 John Wiley & Sons, Ltd.

KEYWORDS: strontium titanate; metastable impact electron spectroscopy (MIES); UPS; STM; AFM; *ab initio* calculations

INTRODUCTION

Surfaces of $SrTiO_3$ single crystals are investigated intensively because of their importance for high-temperature oxygen sensors, in photocatalysis, as substrates for high-T_c superconductors and as dielectric material.[1–5] Most studies up to now have been concerned with non-polar (100) surfaces. During heat treatment in oxygen-rich atmospheres, SrO phases appear on top of these surfaces.[4,6–10] Under reducing conditions Ti–O-containing islands were observed on $SrTiO_3$(100) surfaces.[4,10–12] The composition and number of these islands depend on the oxygen partial pressure and on the dopant concentration, and both factors were described successfully using point defect chemistry models.

Up to now, polar $SrTiO_3$(110) surfaces have not been investigated a great deal. Brunen *et al*. examined undoped $SrTiO_3$(110) single-crystal surfaces heated to ~1000 °C in ultrahigh vacuum for different durations.[13] According to their scanning tunnelling microscopy (STM) results, the surfaces display TiO_2(100) and TiO_2(010) microfacetted planes resulting from the desorption of Sr from the SrTiO-terminated surface.[13] A schematic illustration of the ideal reconstructed surface is shown in Fig. 1. The removal of Sr and O leads to the (1×1) periodicity in Fig. 1(b). The removal of additional Sr, Ti and O leads to the reconstruction with (1×2) periodicity shown in Fig. 1(c). The spacing between the rows amounts to 0.55 nm ($=\sqrt{2} \times 0.391$ nm) for the (1×1) periodicity and 1.1 nm for the (1×2) periodicity. In the [001] direction both reconstructions possess the same periodicity as the $SrTiO_3$(110) surface. These reconstructions are observed regularly and they depend on heating temperature and duration. This will be discussed in the results section.

During STM measurements, the electron tunnelling from the STM tip into partially unoccupied surface orbitals is observed on top of the rows at low bias voltages. This means that the Ti 3d states contribute to the electron tunnelling. Auira *et al*. observed, for $SrTiO_3$(110) surfaces heated at 1000 °C, similar reconstructions accompanied by electron states near the Fermi level (E_F).[14] After heating at 950 °C in ultrahigh vacuum two additional XPS Ti 2p emission peaks were observed that were attributed to ionization from Ti^{3+} 2p and Ti^{2+} 2p states, respectively. The Ti^{3+} 2p emission was attributed to oxygen vacancies whereas the Ti^{2+} 2p emission was attributed to TiO located on top of the TiO_2 microfacets.[14] Similar observations also have been made during heating at 1200 °C in ultrahigh vacuum.[15] Annealing for extended periods at higher temperature leads to the formation of holes and islands on these surfaces. The composition of the islands under ultrahigh vacuum conditions and the underlying formation mechanisms are not well understood and will not

*Correspondence to: W. Maus-Friedrichs, Institut für Physik und Physikalische Technologien, Technische Universität Clausthal, Leibnizstr. 4, D-38678 Clausthal-Zellerfeld, Germany.
E-mail: wmf@physik.tu-clausthal.de
Contract/grant sponsor: Deutsche Forschungsgemeinschaft; Contract/grant number: Ma 1893/2; Bo 532/47.
Contract/grant sponsor: Volkswagen-Stiftung; Contract/grant number: ZN 1354.

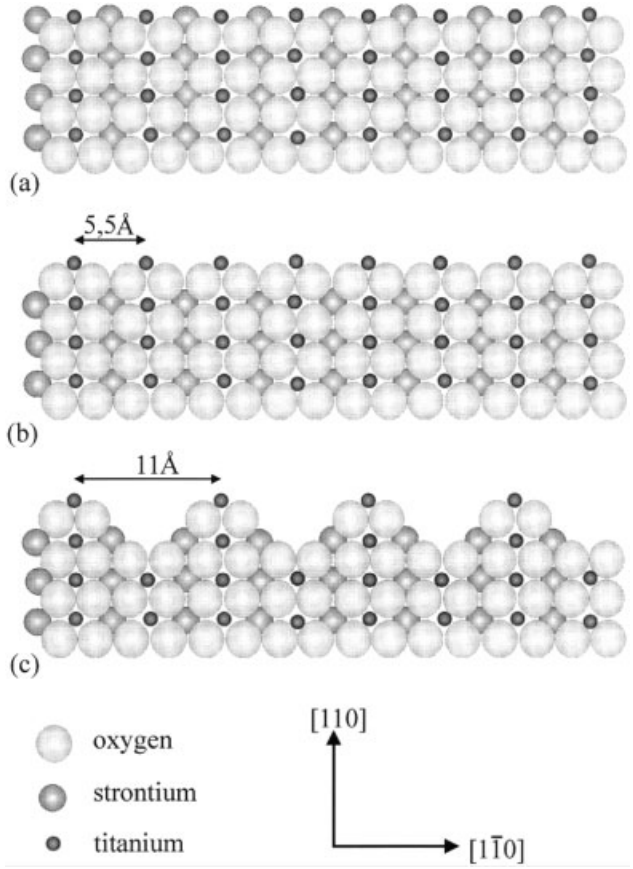

Figure 1. Schematic representation (top view) of the ideal (a) and microfacetted $SrTiO_3(110)$ surface with (1×1) periodicity (b) and (1×2) periodicity (c); side view in [001] direction.

be discussed here. Under oxidizing conditions SrO islands are formed on top of the (110) surfaces.[16] These are similar in composition to those observed on (100) surfaces, but oriented perpendicular to the TiO rows and thus minimize the misfit of the two crystal lattices ($d_{SrO} = 0.51$ nm).

Up to now the TiO termination of the rows has not been confirmed directly. We employed metastable impact electron spectroscopy (MIES), combined with UPS (He(I)), in order to investigate the surface electronic structure of the TiO_2 rows on heated $SrTiO_3(110)$ surfaces. The MIES is well suited for such investigations owing to its extremely high surface sensitivity. In addition, STM and atomic force microscopy (AFM) were applied to obtain information on the topology of the surface studied with MIES. We compare results for $SrTiO_3(110)$ surfaces heated under reducing conditions in ultrahigh vacuum and under oxidizing conditions in synthetic air, respectively. The density of states (DOS) of $SrTiO_3(110)$ surfaces was obtained from *ab initio* Hartree–Fock calculations with different terminations and compared with the experimental MIES and UPS spectra.

EXPERIMENTAL

The measurements were performed using two different set-ups. Both MIES and UPS (He I) were recorded in an ultrahigh vacuum as described in detail previously.[17–19] A time-of-flight technique is used to separate the electrons emitted in the interaction of He^* atoms and He(I) photons with the surface. The electron spectra were recorded with a resolution of 250 meV under normal emission within 100 s. The angle of incidence for the mixed He^*/He(I) beam is 45°. The MIES spectra are displayed as a function of the electron binding energy E_B with respect to the Fermi level E_F.

The STM and AFM measurements were performed in a second apparatus under ultrahigh vacuum conditions with a base pressure below 1×10^{-9} mbar in the main chamber and 4×10^{-10} mbar in the microscope chamber. It is equipped with a commercial AFM/STM system (Omicron).

Commercially available $SrTiO_3$ (denoted by STO) monocrystals (Crystec, Berlin) cut in the (110) direction were heated in a vacuum and in synthetic air, respectively. To remove surface contaminants, the crystals used in the experiments under reducing conditions were annealed at 750 °C for 20 h at pressures below 10^{-8} mbar. Afterwards, the purity level of the surface was determined using MIES and XPS. The crystals heated in synthetic air (80% N_2, 20% O_2) at ambient pressure were cleaned by heating at 750 °C for 20 min after introduction into the vacuum. The target temperatures were controlled by an optical pyrometer (Impac IGA 120) through view ports in both sets of apparatus. The heating procedures in the AFM/STM and the MIES/UPS apparatus were reproduced with a precision of better than 10 K, respectively. All measurements were performed at room temperature.

We present our MIES and UPS results together with those of the *ab initio* calculations. Before discussing the results in detail, some remarks concerning the interaction of He^* with surfaces might be useful: metastable $He^*(2^3S)$ atoms interact with the surfaces via various processes and three different processes may occur (for further details see Refs 20 and 21):

(1) On pure STO surfaces the impinging He^* atoms are ionized by a resonant electron transfer into localized Ti^{3+} 3d surface orbitals. Subsequently the remaining He^+ is neutralized in front of the surface by Auger capture, whereby a surface electron fills the He 1s orbital, emitting a Ti^{3+} 3d electron. Owing to the fact that the Ti 3d orbital possesses a rather small full width at half-maximum (FWHM), the resulting MIES spectrum looks quite similar to an Auger de-excitation spectrum (see below), but is shifted towards lower kinetic energies (i.e. to higher binding energies) by 1.2 eV.[19]
(2) For work functions below ~3.5 eV, Auger de-excitation becomes the dominating process. In this process a surface electron fills the He 1s orbital and the He 2s electron is emitted, carrying the excess energy. The energy balance is similar to UPS with the exception of the different excitation energy (19.8 eV for He^* 2^3S).
(3) For work functions below ~2.2 eV and a high electron density just below the E_F the probability for resonant electron transfer from the surface to He^* becomes sizeable, forming He^{-*} 1s $2s^2$ ions in front of the surface.[22] These species decay rapidly in an intra-atomic autodetachment process.

We present our results as a function of the binding energy E_B, with respect of E_F of the electrons emitted in

the Auger de-excitation process. In the case of the clean STO(110), the defect-modified Auger capture process is the dominating interaction mechanism in MIES. As discussed above, however, the resulting spectra are nevertheless quite similar to those from Auger de-excitation.[19]

COMPUTATIONAL DETAILS

In the present study, the STO(110) surface has been modelled using a *slab model*. In this model, the crystal is considered as a set of seven crystalline planes parallel to the (110) surface; such a slab has a finite thickness but is periodic in the surface plane. To avoid problems with cluster boundary conditions we use a periodic seven-plane slab model of a film infinite in two dimensions. This model in the framework of the Hartree–Fock approach was employed successfully in surface and interface studies.[23] To perform *ab initio* calculations of the (110) surface we use the Hartree–Fock formalism as implemented into the Crystal-98 computer code,[24–26] which was widely and successfully used in recent years for modelling solids and surfaces,[27–31] including interpretation of MIES data.[18,32] This code has the unique feature of simulating an isolated purely two-dimensional slab without artificial periodicity in the direction perpendicular to the surface.

The crystalline orbitals used in Hartree–Fock calculations as the basis set for the wavefunction expansion are constructed from a linear combination of atom-centred Gaussian orbitals (HF-LCGO approximation). Thus, the correct choice of basis set is an important step in *ab initio* calculations. In our simulations, we use the all-electron basis set for both O and Ti atoms: 8(s)–411(sp) and 8(s)-6-411(sp)-31(d), respectively.[26] For the purpose of reducing the computational efforts for heavy Sr atoms, we employed a small-core Hay–Wadt pseudo-potential.[33–35] The initial guess for the Sr basis set 31(sp)-3(d) has also been taken from Ref. 26 and then has been re-optimized for a strontium titanate crystal. To test how these basis sets reproduce the main experimentally observable bulk properties, the lattice constant a_0 and the bulk modulus B have been calculated. We obtained $a_0 = 3.93$ Å and $B = 211$ GPa, which only slightly overestimate the experimental values (extrapolated to 0 K): $a_0 = 3.89$ Å and $B = 179$ GPa.[36] These results allowed us to conclude that the HF-LCGO method can be considered good enough to describe the electronic structure of STO surfaces. It should be noted also that to achieve high accuracy in the calculations large tolerances were employed for evaluation of the infinite overlap, Coulomb and exchange series.[25] The reciprocal space integration was performed by a sampling of the Brillouin zone with the $8 \times 8 \times 8$ Pack–Monkhorst net,[37] which provides a balanced summation in direct and reciprocal lattices.[38]

The $SrTiO_3$ surface in the (110) direction consists of a sequence of alternating charged SrTiO and O_2 planes. It is also well known that such a surface is unstable owing to an infinite dipole moment produced by the charged planes perpendicular to the surface. This is why cleavage of this surface should result in the formation of one of the two stable surfaces: Sr-terminated and TiO-terminated.[39] In our calculations, we simulated a TiO-terminated surface and its reduction to a Ti-terminated surface when all O atoms are removed from the first plane (Fig. 1(b)). To compare our calculations with the MIES experiments, we compare the DOS projected on the first plane (TiO or Ti-terminated) and the effective charges of atoms in the slab, as well as the electron populations of Ti atoms in different situations. The calculated DOS is convoluted with a Gaussian function to account for the electron–phonon broadening of the electron emission spectra and the experimental resolution.[18] A value of 1 eV was chosen for the width of the Gaussian because it gives good agreement between calculated DOS and UPS spectra.

RESULTS AND DISCUSSION

An STM image ($10 \times 10\,nm^2$) of the $SrTiO_3(110)$ surface annealed at 1000 °C in ultrahigh vacuum for 1 h is shown in Fig. 2. The surface appears to be restructured during the heating procedure. A reconstruction is observed, indicated by the lines added to the image. The mean distance between these lines amounts to ~5.4 Å. This value corresponds well to the (1×1) microfacet formation observed previously.[13–15] No islands could be found on top of these surfaces at annealing durations of <3 h.

Figure 3 shows an AFM image ($10 \times 10\,nm^2$) of the $SrTiO_3(110)$ surface heated to 900 °C in synthetic air for 1 h. The entire surface appears to be restructured more uniformly than that in Fig. 2. The (1×1) and (1×2) reconstruction is evident. The distance between the two neighbouring rows in the image was found to be 5.4 nm and 10.8 Å, respectively. These values correspond well to the microfacet reconstruction, which consists of parallel rows with distances of ~5.5 Å or 11.0 Å (see Fig. 1).[13–15] Again, owing to the mild and short-timed heating treatment, no islands could be found on this surface.

The MIES spectra of the clean and unreconstructed surface are shown in Fig. 4(a), together with spectra of the surfaces after heating in air at 900 °C for 1 h and in a vacuum at 1000 °C for 1 h, respectively. The MIES spectra are compared with the calculated DOS projected (PDOS) on the Ti 3d orbitals of the reconstructed surface (corresponding to Fig. 1(b)).

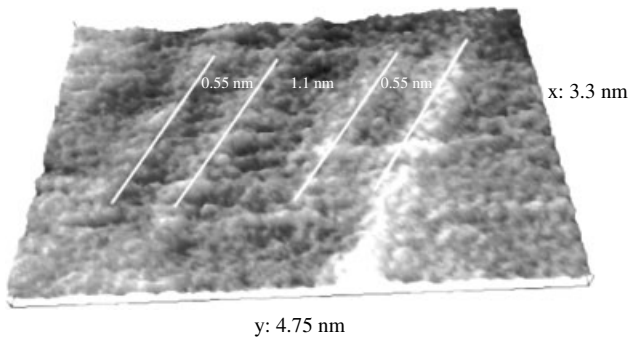

Figure 2. The STM image ($6 \times 10\,nm^2$) of the $SrTiO_3(110)$ surface heated to 1000 °C for 1 h in ultrahigh vacuum (+1 V, 0.1 nA). The lines indicate the ridge tops.

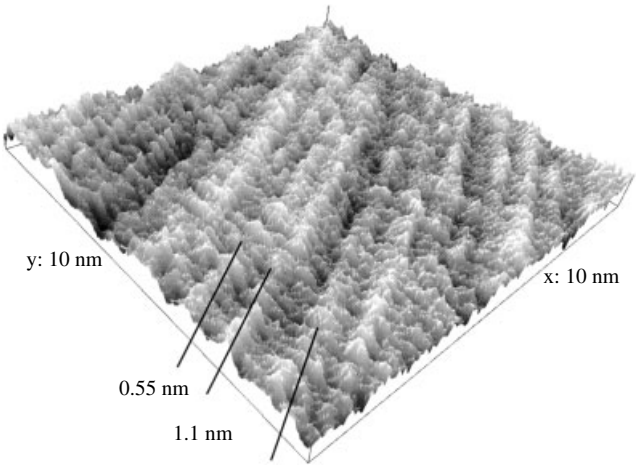

Figure 3. The AFM image (10×10 nm^2) of the $SrTiO_3(110)$ surface heated to 900 °C for 1 h in synthetic air (20% O_2, 80% N_2).

The UPS spectra of the clean STO(110) heated in a vacuum at 1000 °C for 1 h and the clean and unreconstructed STO(110) are shown in Fig. 4(b). Also plotted in this figure are the PDOS projected to the first plane of the TiO-terminated slab of the unreconstructed surface (corresponding to Fig. 1(a)), projected on the Ti 3p orbitals and projected on the Ti 3d orbitals belonging to the first layer atom.

The MIES and UPS spectra of the clean unreconstructed (110) surface are similar to those of $SrTiO_3(100)$:[10,11,19] a dominant structure denoted by O 2p appears at $\sim E_B = 7$ eV from the ionization of O 2p orbitals. In contrast to MIES, the UPS (He (I)) spectra display a double-peak structure in this region. As shown in our previous work on MgO,[18] STO(100)[36] and Al_2O_3,[32] MIES is particularly sensitive to orbitals protruding out of the surface. Here, this results in a higher probability for the detection of O 2p orbitals directed perpendicular to the surface. The MIES and UPS spectra of the surface heated in a vacuum show additional peaks near zero binding energy. The same surface heated in synthetic air does not show similar features being investigated without any treatment. But applying a mild heating procedure (750 °C for 10 min) the additional peak near E_F is found. This treatment is not sufficient for any surface reconstruction. It is therefore likely to assume that the discussed reconstruction also takes place during heating in synthetic air, but immediately the top surface rows are covered by weakly bound oxygen atoms arising from the air. To examine this assumption we offered oxygen to a cleaned surface in an ultrahigh vacuum: an oxygen exposure of 1 L (1 Langmuir $= 1 \times 10^{-6}$ Torr × s) is already sufficient

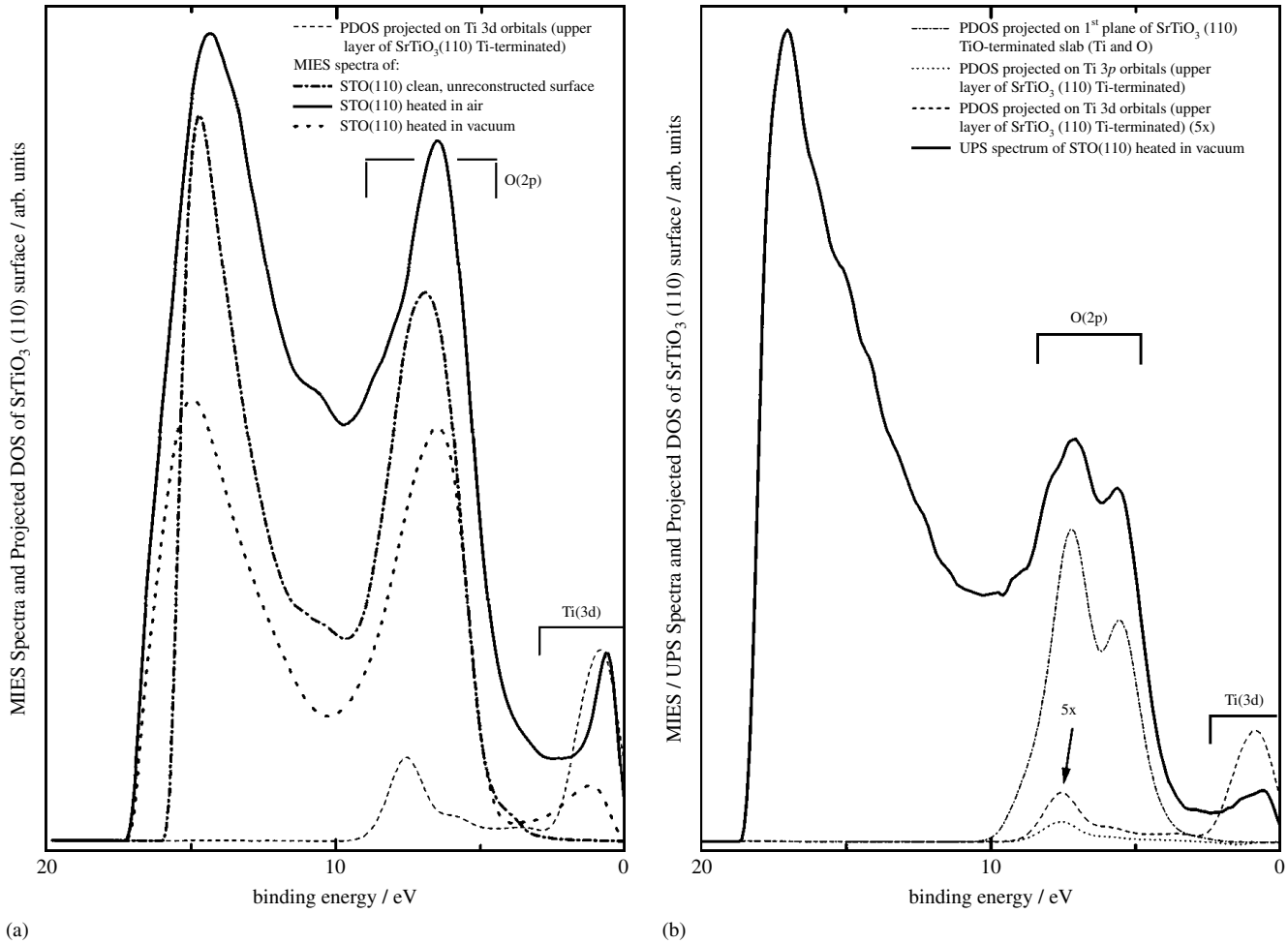

Figure 4. The MIES, UPS and *ab initio* DOS results for the clean unreconstructed and heated $SrTiO_3(110)$ surfaces. See text and inserts for detailed description.

to remove this peak completely. Again, the mild heating procedure (750 °C for 10 min) at low temperatures recovers the features near E_F completely.

The emissions detected beyond about $E_B = 10$ eV are attributed to secondary electrons and are not discussed here.

In our calculations we used an orientation where the *x*-direction was selected parallel to the surface and the *y*- and *z*-axes were oriented to the surface with an angle of 45°. The DOS projected onto the topmost plane is also shown in Fig. 4(b). For the Ti-terminated surface, contributions of the Ti 3p and Ti 3d states are shown separately. Tables 1 and 2 give atomic charges and electron occupancies of the Ti atomic orbitals in different planes of both surface terminations. Theory is able to reproduce the double-peak structure from the O 2p states seen with UPS. Positions and shapes of the O 2p emission in the DOS and UPS spectra agree well. The peak at lower binding energies ($E_B = 5.8$ eV) involves the contributions of 2p orbitals oriented perpendicular to the surface whereas that at the larger binding energies stems from orbitals parallel to the surface. The reproduction of the double-peak structure shows that UPS (He (I)), in the present case, mainly images the DOS of the initial states. We found that the reasons for the MIES sensitivity were mainly due to contributions from the O 2p emission perpendicular to the surface. Thus, MIES possesses a higher sensitivity for the detection of initial states at the STO surface with p_{yz} character. These partial DOS have projections directed perpendicular to the (110) surface. The superposition of the DOS contributions from differently oriented O 2p orbitals combined with the different sensitivity for the detection of p_{yz} and p_x orbitals produces a broad single peak in MIES, rather than the double-peak structure seen in UPS (He (I)). The reconstructed (110) surface shows a very similar O 2p contribution in the UPS spectra.

In addition, a novel peak is observed near zero binding for the reconstructed surface energy in the DOS. The calculations establish that the Ti 3d states become populated during reconstruction of the surface and are responsible for the DOS contribution near zero binding energy; 3p orbitals yield only a small contribution around 7 eV. The good agreement in shape and position between DOS and MIES spectra suggests that MIES directly images the DOS of the initially populated Ti 3d states of the surface via the Auger de-excitation process.

The values in Tables 1 and 2 confirm these conclusions. Owing to the Ti–O chemical bond covalence, the effective charges (*e*) of Ti and O atoms in the bulk differ considerably from the ionic model (+4 *e* and −2 *e*, respectively), unlike the charge of the Sr ions (1.9 *e* instead of 2 *e*). At the TiO-terminated surface, the Ti ion charge (2.46 *e*) does not differ considerably from that in the central, third plane of a slab simulating the bulk (2.56 *e*). The O ion charges at the TiO surface and in the slab centre are also close (−1.29 *e* vs. −1.57 *e*). In contrast, compared with the TiO surface, the Ti effective charge is decreased by ~1 *e* at the Ti-terminated surface (1.45 *e* vs. 2.46 *e*). This is accompanied by a strong increase in the population of the Ti 3d orbitals, from 1.29 *e* to 2.49 *e*. Indeed, these Ti 3d orbitals give the main contribution to the MIES peak around 1 eV below E_F.

Summarizing, the present study constitutes one of the rare cases where, at the same time, the topological and electronic properties of a surface were characterized successfully by both *ab initio* calculations and sophisticated spectroscopic and microscopic experiments.

Table 1. Effective Mulliken charges, *Q* (*e*), for two different $SrTiO_3(110)$ terminations (bulk charges of ions: Sr = 1.905, Ti = 2.558 and O = −1.488)

		Effective charge for different terminations	
Layer	Atoms	TiO	Ti
1	Ti	2.457	1.452
	O	−1.387	
2	O	−1.288	−1.427
3	Sr	1.874	1.848
	Ti	2.561	2.581
	O	−1.481	−1.494
4	O	−1.566	−1.427

Table 2. Titanium orbital population for two different $SrTiO_3(110)$ terminations. (Ti orbital populations for a bulk crystal: Ti 3p = 6.003, Ti 3d = 1.226, Ti 4s = 0.160)

		Population for different terminations	
Layer	Orbitals	TiO	Ti
	Ti 3p	6.026	5.870
1	Ti 3d	1.292	2.488
	Ti 4s	0.171	0.123
	Ti 3p	6.022	6.011
3	Ti 3d	1.201	1.194
	Ti 4s	0.165	0.162

SUMMARY

Short-time heating of $SrTiO_3(110)$ at temperatures of 900 °C results in a microfacetting of the surface observed with AFM and STM. Rows are formed with (1 × 1) or (1 × 2) periodicity. The electronic structure of the surfaces was studied by MIES and UPS (He I); the results are compared with *ab initio* Hartree–Fock calculations also presented in this paper. Besides giving good overall agreement with the observed O 2p emission, the calculations identify an additional peak close to zero binding energy for the heated, Ti-terminated surface as being due to Ti 3d occupied states, giving direct evidence for the termination of the reconstructed, microfacetted surface by reduced Ti species.

Acknowledgements

Financial support by the Deutsche Forschungsgemeinschaft under contracts Ma 1893/2 and Bo 532/47, by the Volkswagen-Stiftung for Israel–German cooperation (ZN 1354) and, in part, by the KAMEA programme is gratefully acknowledged. We are thankful to Drs E. Heifets and R. Eglitis for discussions and providing us with the relaxed geometries of the TiO-terminated surfaces.

REFERENCES

1. Ravikumar V, Wolf D, David P. *Phys. Rev. Lett.* 1995; **74**: 174.
2. Stäuble-Pümpin B, Ilge B, Matjasevic VC, Scholte PMLO, Steinfort AJ, Tuinstral F. *Surf. Sci.* 1996; **369**: 313.
3. Liand Y, Bonnell DA. *Surf. Sci. Lett.* 1993; **285**: L510.
4. Szot K, Speier W, Herion J, Freiburg Ch. *Appl. Phys. A* 1997; **64**: 55.
5. Lopez A, Heller T, Bitzer T, Chen Q, Richardson NV. *Surf. Sci. Lett.* 2001; **494**: L811.
6. Szot K, Speier W. *Phys. Rev. B* 1999; **60**: 5909.
7. Szot K, Speier W, Breuer U, Meyer R, Szade J, Waser R. *Surf. Sci.* 2000; **460**: 112.
8. Wei H, Beuermann L, Helmbold J, Borchardt G, Kempter V, Lilienkamp G, Maus-Friedrichs W. *J. Eur. Ceram. Soc.* 2001; **21**: 1677.
9. Wei H, Maus-Friedrichs W, Lilienkamp G, Kempter V, Helmbold J, Gömann K, Borchardt G. *J. Electroceram.* 2002; **8**: 221.
10. Gunhold A, Gömann K, Beuermann L, Frerichs M, Borchardt G, Kempter V, Maus-Friedrichs W. *Surf. Sci.* 2002; **507–510**: 447.
11. Gunhold A, Beuermann L, Frerichs M, Kempter V, Gömann K, Borchardt G, Maus-Friedrichs W. *Surf. Sci.* 2002; **523**: 80.
12. Gunhold A, Gömann K, Beuermann L, Kempter V, Borchardt G, Maus-Friedrichs W. *Anal. Bioanal. Chem.* 2003; **375**: 924.
13. Brunen J, Zegenhagen J. *Surf. Sci.* 1997; **389**: 349.
14. Auira Y, Bando H, Nishihara Y, Haruyama Y, Kodaira S, Komeda T, Sakisaka Y, Maruyama T, Kato H. In *Advances in Superconductivity VI*, Fujita T, Shiohara Y (eds). Springer Verlag: Tokyo, 1994; 983.
15. Bando H, Auira Y, Haruyama Y, Shimuzu T, Nishihara Y. *J. Vac. Sci. Technol. B* 1995; **13**: 1150.
16. Gömann K, Borchardt G, Gunhold A, Maus-Friedrichs W, Beuermann L, Kempter V, Lesage B, Kaitasov O, Baumann H. *Mater. Res. Soc. Proc.* 2003; **375**: E3.1.1.
17. Brause M, Braun B, Ochs D, Maus-Friedrichs W, Kempter V. *Surf. Sci.* 1998; **398**: 184.
18. Ochs D, Maus-Friedrichs W, Brause M, Günster J, Kempter V, Puchin V, Shluger A, Kantorovich L. *Surf. Sci.* 1996; **365**: 557.
19. Maus-Friedrichs W, Frerichs M, Gunhold A, Krischok S, Kempter V, Bihlmayer G. *Surf. Sci.* 2002; **515**: 499.
20. Morgner H. *Adv. At. Mol. Opt. Phys.* 2000; **48**: 387.
21. Harada Y, Masuda S, Ozaki H. *Chem. Rev.* 1997; **97**: 1897.
22. Hemmen R, Conrad H. *Phys. Rev. Lett.* 1991; **67**: 1314.
23. Heifets E, Eglitis R, Kotomin E, Maier J, Borstel G. *Phys. Rev. B* 2001; **64**: 23 514.
24. Pisani C. *Quantum Mechanical Ab-initio Calculations of the Properties of Crystalline Materials*, vol. 67 of Lecture Notes in Chemistry. Springer Verlag: Berlin, 1996.
25. Saunders VR, Dovesi R, Roetti C, Causa M, Harrison NM, Orlando R, Zicovich-Wilson CM. *CRYSTAL'98 User's Manual*. Universita di Torino: Torino, 1998.
26. http://www.chimifm.unito.it/teorica/crystal/crystal.html
27. http://www.cse.clrc.ac.uk/cmg/crystal
28. Towler MD, Zupan M, Causa M. *Comput. Phys. Commun.* 1996; **98**: 181.
29. Dovesi R, Orlando R, Roetti C, Pisani C, Saunders VR. *Phys. Status Solidi B* 2000; **217**: 63.
30. Doll K, Saunders VR, Harrison NM. *Int. J. Quant. Chem.* 2001; **82**: 1.
31. Civalleri B, D'Arco P, Orlando R, Saunders VR, Dovesi R. *Chem. Phys. Lett.* 2001; **348**: 131.
32. Puchin VE, Gale JD, Shluger AL, Kotomin EA, Günster J, Brause M, Kempter V. *Surf. Sci.* 1997; **370**: 190.
33. Hay PJ, Wadt WR. *J. Chem. Phys.* 1984; **82**: 270.
34. Hay PJ, Wadt WR. *J. Chem. Phys.* 1984; **82**: 284.
35. Hay PJ, Wadt WR. *J. Chem. Phys.* 1984; **82**: 299.
36. Hellwege KH, Hellwege AM. *Ferroelectrics and Related Substances*, vol. 3 of New Series. Landolt-Bornstein, group III. Springer Verlag: Berlin, 1969.
37. Monkhorst HJ, Pack JD. *Phys. Rev. B* 1976; **13**: 5188.
38. Bredow T, Evarestov RA, Jug K. *Phys. Status Solidi B* 2000; **222**: 495.
39. Heifets E, Kotomin EA, Maier J. *Surf. Sci.* 2000; **462**: 19.